DESY HERA 95-04
April 1995

Study of Background Caused by Scattering at the HERA-B Wire Target

E. Lohrmann, M. Seidel

Deutsches Elektronen Synchrotron DESY
Hamburg

1. Overview

The HERA-B experiment requires a very high interaction rate of beam halo protons, the design value being 40 MHz. Tests with a prototype wire target at a position near the primary proton collimator in the West straight section were carried out in 1994. They produced, under certain operating conditions, a large background in the ZEUS experiment. This indicates that stray radiation, produced at the HERA-B wire target, can directly hit the ZEUS experiment. This note describes a possible reason and suggests measures to minimize this background at the HERA experiments.

2. Scattering on a Thin Target

Particles hitting the wire target can interact or undergo a (quasi) elastic scattering. If the scattering angle is large enough, they will get lost at aperture restrictions, resulting in background at the experiments. Since we are only interested in large scattering angles and large effects, it suffices to consider single (quasi) elastic scattering. Absorption and scattering of high energy protons or neutrons on nuclei have been studied extensively [1, 2, 3]. The results are briefly the following:

At high energies >10 GeV cross sections depend only weakly on energy. The total cross section of protons or neutrons impinging on nuclei with atomic number A > 7 is with sufficient accuracy given by

$$\sigma_T(pA) = 46\,\text{mb} \cdot A^{0.79}. \qquad (1)$$

A list of cross sections is given in table 1, valid for neutrons at about 200 GeV.

nucleus	σ_T (mb) [1]	σ_{inel} (mb) [2]
^{9}Be	264	199
^{12}C	331	237
^{27}Al	628	430
^{56}Fe	1100	721
^{63}Cu	1213	794
^{113}Cd	1884	1196
^{184}W	2840	1691
^{208}Pb	3000	1808

Table 1: Cross sections of selected nuclei, σ_T = total, σ_{inel} = inelastic cross section.

The elastic cross section can be taken from table 1:

$$\sigma_{el} = \sigma_T - \sigma_{inel}.$$

The ratio σ_{el} / σ_T can be parametrized by

$$\frac{\sigma_{el}}{\sigma_T} = 0.205 \cdot A^{0.13} \qquad (2)$$

with an accuracy of a few percent.

The elastic nuclear scattering is described to a very good approximation by diffraction on a grey disc. If the absorbing nuclear matter has a gaussian density distribution, then the scattering differential cross section is also gaussian. For our purposes this is a sufficiently good approximation.

The elastic differential cross section is then:

$$\frac{d\sigma}{d\Omega} = \sigma_0 \cdot exp\left(-\mathrm{B(A)} \cdot p_t^2\right) \qquad (3)$$

with the transverse momentum

$$p_t = p \cdot sin(\theta)$$

and $\qquad p$ = proton beam momentum.

The parameter σ_0, i.e. the forward differential cross section, is related to the to the total cross section σ_T by the optical theorem:

$$\sigma_0 = \frac{\sigma_{\mathrm{T}}^2 p^2}{16\pi^2\hbar^2}. \qquad (4)$$

The total elastic cross section is obtained by integration of equation (3), with equation (4):

$$\sigma_{\mathrm{el}} = \frac{\sigma_{\mathrm{T}}^2}{16\pi\,\mathrm{B(A)}\hbar^2} \qquad (5)$$

From equations (1), (2) and (5) we can determine the parameter B(A):

$$\mathrm{B(A)} = 11.5 \cdot \mathrm{A}^{0.66}\,(\mathrm{GeV/c})^{-2}. \qquad (6)$$

This can be related to the rms nuclear radius

$$\mathrm{R} = 2\hbar\sqrt{\mathrm{B(A)}} = 1.34 \cdot \mathrm{A}^{0.33}\ \mathrm{fm}.$$

The rms scattering angle is

$$\left\langle \theta^2 \right\rangle^{\frac{1}{2}} = \frac{1}{p\sqrt{\mathrm{B(A)}}}. \qquad (7)$$

For a Cu-target at p = 820 GeV we have thus

$$\left\langle \theta^2 \right\rangle^{\frac{1}{2}} = 92\,\mu\mathrm{rad}$$

and for Al:

$$\left\langle \theta^2 \right\rangle^{\frac{1}{2}} = 120\,\mu\mathrm{rad}.$$

Projected into the *xz*- or *yz*- plane the rms scattering angles are 65 μrad for Cu and 85 μrad for Al.

For a more careful evaluation one has to consider also incoherent elastic scattering on individual nucleons insight the nucleus. This cross section is [3]:

$$\left(\frac{d\sigma}{d\Omega}\right)^{incoh} = 44\,\text{mb}\ A^{0.33} \left(\frac{p}{\text{GeV}/c}\right)^2 exp\left(-B(1)\cdot p_t^2\right) \tag{8}$$

with $B(1) = 10(\text{GeV}/c)^{-2}$ and p inserted in GeV/*c*.
The coherent and incoherent QED scattering cross sections are:

(i) coherent:

$$\frac{d\sigma}{d\Omega} = \frac{4Z^2\alpha^2\hbar^2}{p^2\theta^4} exp\left(-B(A)p_t^2\right) \tag{9}$$

(ii) incoherent:

$$\frac{d\sigma}{d\Omega} = \frac{4Z\alpha^2\hbar^2}{p^2\theta^4}\left(1+\frac{p_t^2}{Q_0^2}\right)^{-4}, \qquad Q_o^2 = 0.71\,(\text{GeV}/c)^2. \tag{10}$$

They can be neglected compared to nuclear scattering, for not too small angles.

The quasi elastic cross sections equations (3), (8), (9), (10) for coherent and incoherent nuclear scattering and for coherent and incoherent QED scattering have been integrated with the help of equations (1), (4), (6) for Cu and Al targets and a proton energy of 820 GeV. In fig. 1 the result is shown in the form

$$r(\theta_p) = \frac{1}{\sigma_T}\int_{\theta_p}^{+\pi} d\theta_x \int_{-\pi}^{+\pi} d\theta_y \left(\frac{d\sigma}{d\Omega}\right) = \frac{\sigma_{el}(>\theta_p)}{\sigma_T} \quad . \tag{11}$$

Here r is the probability per nuclear collision to obtain an elastic scattering at a projected angle $>\theta_p$.

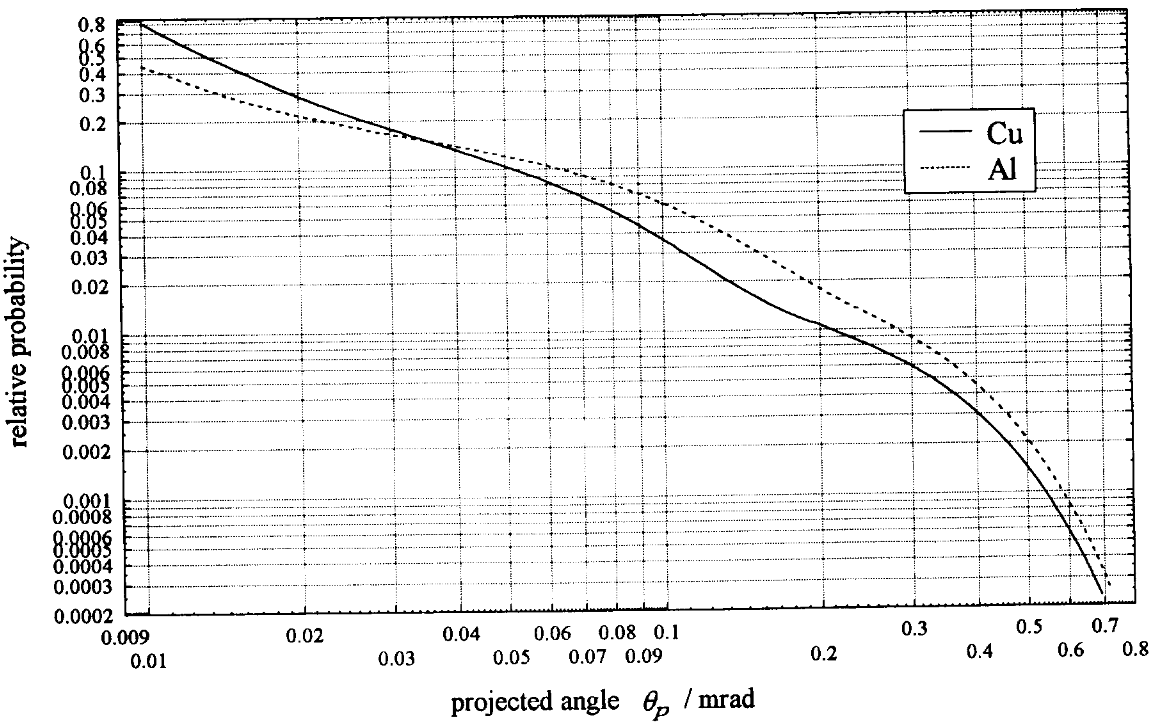

Fig. 1: Relative probabilities for the occurrence of elastic scattering angles $>\theta_p$, projected into one plane.

3. The 1994 Experimental Setup

One may ask now if the observed increased loss rates at ZEUS can be explained with the elastic cross sections discussed above. At present the wire target is located at WR118m, not far from the primary collimator at WR111m. In fig. 2 horizontal phase space ellipses corresponding to the amplitudes of the target (7σ), the collimators (9σ) and the aperture restriction (11σ) are shown, rescaled to the target position. The assumed amplitudes are based on a horizontal emittance[1] of $\varepsilon_x = 6 \cdot 10^{-3}$ mm mrad. The half aperture of 11σ in the QR-magnets next to the interaction regions is about the maximum achievable value and therefore somewhat optimistic.

If one considers only small angle coulomb scattering, halo protons with amplitudes between the target and collimator position will hit the target many times and will undergo a relatively slow emittance growth. When these particles reach an amplitude, defined by the collimator, they will be removed from the beam with a high efficiency during a small number of revolutions. However, in case of hard elastic scattering particles can jump immediately to an amplitude outside the machine aperture. The necessary projected scattering angle can be calculated from

$$|\theta| > \sqrt{\frac{\varepsilon}{\beta_t}\left(n_a^2 - n_t^2\right)}, \qquad (12)$$

where β_t is the amplitude function at the target position, n_a is the half aperture in units of σ and n_t the amplitude defined by the target.

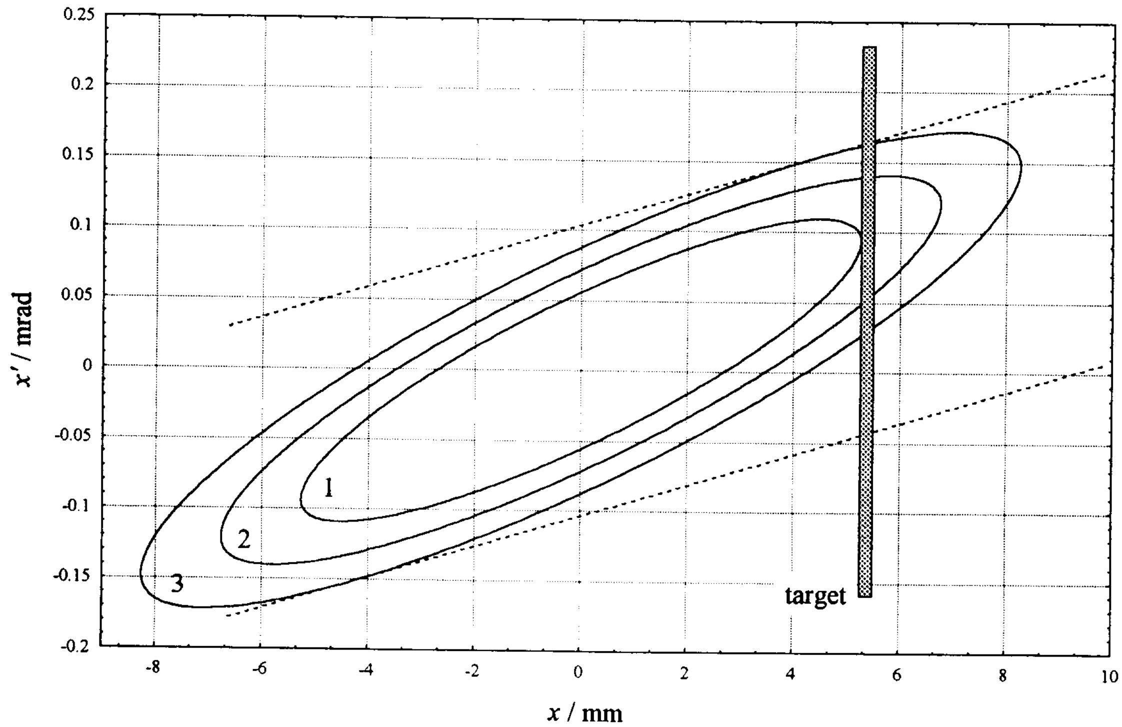

Fig. 2: Phase space limitations at the target position in the horizontal plane. The ellipses correspond to particle amplitudes limited by the target (1), the collimators (2) and the aperture limit (3). The target is indicated with its real transverse width of 250 μm.

[1] This emittance corresponds to 1σ of a two dimensional gaussian distribution or 39.3 % of the particles.

Particles outside the aperture limited ellipse have still a chance to pass through the aperture limits at ZEUS, H1 and could be captured by the collimators in the next turn. In particular that depends on the phase difference between target and aperture restriction. The dotted lines in fig. 2 indicate the aperture limit in the QR-quadrupole, upstream of ZEUS, projected to the target position. Taking into account the phase advance, the necessary scattering angle at the target for a hit at the aperture limit is given by [6]

$$|\theta| > \sqrt{\frac{\varepsilon}{\beta}} \cdot \left| \frac{n_t \cos(\Delta\varphi) \pm n_a}{\sin(\Delta\varphi)} \right|, \qquad (13)$$

where $\Delta\varphi$ is the phase difference between target and aperture restriction. With the help of the integrated angular distribution in fig. 1 and the equations (12), (13) it is now possible to estimate the scattering angles and the probabilities for general crossing of the acceptance and for a hit of the aperture at ZEUS after hard elastic scattering in the target. The results are given in table 2.

	horizontal		vertical	
	θ_x / µrad	P	θ_y / µrad	P
crossing of acceptance	±67.8	0.14	±104	0.066
hit in QR/QS magnet	+68.9, -136.1	0.088	+3290, -712	0.0001

Table 2: Scattering angles θ_x, θ_y and probabilities P per nuclear collision in the target for acceptance crossing and hits in the ZEUS QR/QS magnet after hard elastic scattering at a copper target. The numbers for the vertical plane are based on an emittance of $\varepsilon_y = 4.5 \cdot 10^{-3}$ mm mrad and on the same relative amplitudes of target, collimators and aperture as in x.

A more precise estimate can be obtained by tracking the scattered protons around the machine and finding the individual loss positions, caused either by a hit of an aperture limit or by an inelastic event in the target or in one of the collimator jaws. In table 3 results of such a simulation are given for the cases of having the target on the same side and on the opposite side as the primary collimator, i.e. for a target with and without optimized secondary collimators. In comparison of both cases it is clearly visible that secondary collimators can shadow the scattered protons effectively if they are installed at optimal positions with respect to the target. It should be noted that a particle which touches the beam pipe is assumed to be lost in the simulation whereas in practice the chance of elastic outscattering is certainly not negligible.

1994 setup	target on same side as primary collimator	target on other side
target	12.0 %	10.9 %
collimators	86.45 %	71.3 %
ZEUS (QR/QS upstream)	1.4 %	10.8 %
H1 (QR/QS upstream)	0.05 %	3.65 %
other positions	0.1 %	3.35 %

Table 3: Probabilities for losses obtained from a tracking simulation after a nuclear elastic scattering event in the horizontal target. Note that even in the case that the target is installed on the wrong side, a part of the scattered particles is captured by the secondary collimators in both planes. The estimate in table 2 assumes no collimators at all and takes into account only scattering in one selected plane.

During the 1994 experiments the rate of inelastic events reached often values above $\nu_{inel} = 10\,\mathrm{MHz}$. The rate of elastic events is then given by $\nu_{el} = \sigma_{el} / \sigma_{inel} \cdot \nu_{inel} \approx 6\,\mathrm{MHz}$, and according to the simulation in table 3 the rate of hits in the QR magnet at ZEUS can reach 600 kHz with not optimized collimators. This value is rather high and could easily explain the observed increased background rates.

4. Future Setup and Possibilities to Optimize the Background Conditions at ZEUS and H1

The HERA-B experiment will be installed in the Hall West, using 8 wire targets at 9 m on the upstream side of the hall's symmetry point. At the new target position the β-functions are relatively small (see table 5). The emittance increase which a particle receives due to scattering at the target by an angle θ is given by

$$\Delta\varepsilon = \beta \cdot \theta^2. \qquad (14)$$

Scattering at the new target location therefore leads to a smaller emittance increase and the risk of particle losses is reduced. This can be seen qualitatively in fig. 3 and quantitatively in table 4 in comparison to fig. 2 and table 2 for the old setup. The horizontal phase advance between target and aperture restriction at ZEUS is now close to 180°. Therefore very large scattering angles are necessary for a hit of the ZEUS aperture in the first turn (see dotted lines in fig. 3). However, in this arrangement the required scattering angle depends very sensitively on the phase difference and the optical functions are known only to a typical precision of ~ 5 %. Moreover the general problem is not solved because the phase advance in the vertical plane is not close to 180° and one has to consider also losses at H1. On the other hand one should keep in mind that the phase advance between target and aperture is a parameter which can be optimized in such a way that scattered protons can pass through critical aperture restrictions.

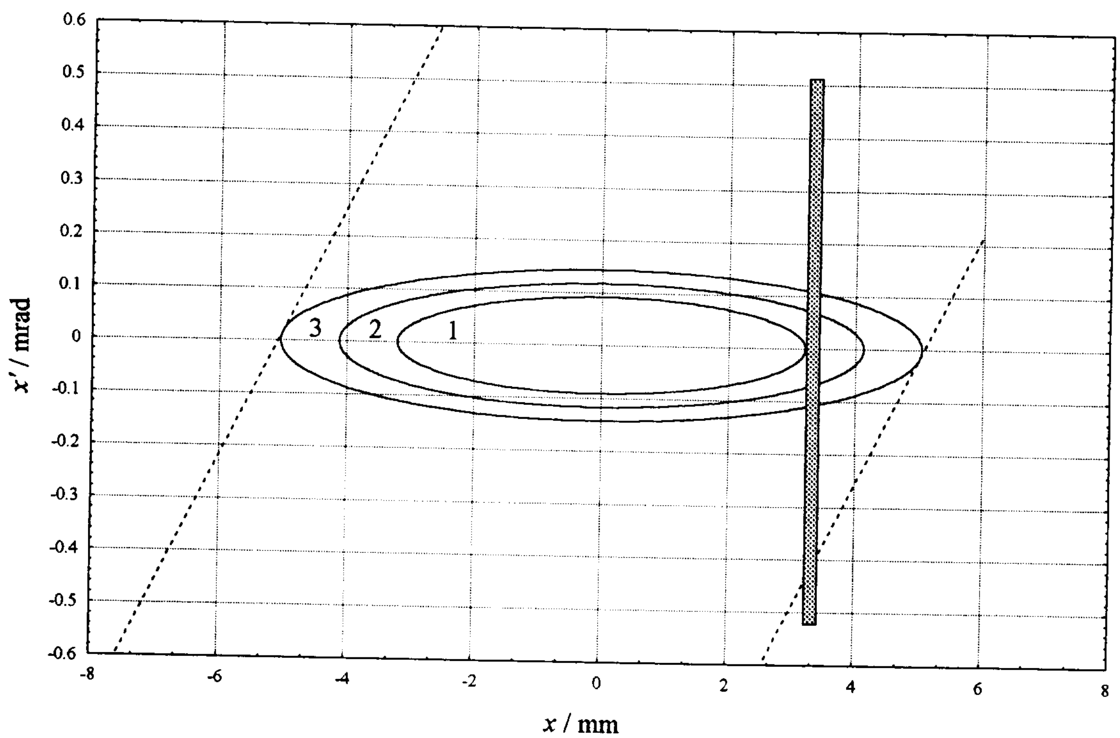

Fig. 3: Phase space limitations in the new setup, projected to the target position at WR009m.

1996 setup	horizontal		vertical	
	θ_x / µrad	P	θ_y / µrad	P
crossing of acceptance	±111	0.06	±96.2	0.086
hit in QR/QS magnet	+445, -1970	0.002	+105, -157	0.048

Table 4: Scattering angles θ_x, θ_y and probabilities P for acceptance crossing and hits of the ZEUS QR/QS magnet in the final HERA-B setup.

Let us consider how the collimators in the proton ring would improve the situation. The special requirements of the HERA-B experiments made it necessary to rearrange a large number of optical elements in the straight section west (see the report of B. Parker [5]). As a result of these changes new positions for the collimators had to be found. It was not possible to move the whole collimation system downstream the HERA-B detector because the phase advance is not large enough in that region. Therefore the primary collimator has to be positioned upstream of the experiment. The phase advances and β functions at the positions of collimators and targets are given in table 5.

1996 setup	Ψ_x / deg	type	β_x / m	Ψ_y / deg	type	β_y / m
KX0, KY0 (WR094)	0	p	140.1	0	p	79.0
KY1 (WR033)	-	-	-	27	s1	48.5
targets (WR009)	121	t	35.0	65	t	35.0
KX1 (WL019)	158	s1, t1	62.3	-	-	-
KX2, KY2 (WL105)	189		162.9	182	t1	104
KX3, KY3 (WL150)	209	s2,(t2)	41.6	311	s2, t2	78.9

Table 5: Beta functions and phase advances at collimators and targets in the straight section west. The type notations have the following meaning: p - primary collimator, t - target, s1, s2 - secondary collimators for the primary collimator, t1, t2 - secondary collimators for the target.

It should be noted that the proposed arrangement of collimators contains some redundancy - both vertical collimators on the west right side can be used as primary ones. After gaining of some practical experience the best combination can be chosen. Furthermore redundant secondary jaws in WL can be used to catch elastically scattered particles from the target. The optimum phase advances of secondary collimators with respect to a scattering target are given by [6]:

$$\Delta\varphi^{\text{opt}} = m \cdot 180^o \pm a\cos\left(\frac{n_t}{n_s}\right), \qquad (15)$$

where m is an integer number and n_t, n_s are the amplitudes of target and secondary collimator in units of beam-sigma respectively. Putting in 7σ and 9σ as an example we find $\Delta\varphi^{\text{opt}} = m \cdot 180^o \pm 40^o$. Looking at table 5 it turns out that for the vertical plane *KY2* and *KY3* are not optimal but can be used as secondary collimators for the target. One could think of moving *KY2* by some degrees downstream, however, this will be difficult because the region is already occupied by quadrupole magnets and furthermore the β-function is very small. With respect to the target *KY3* should be moved upstream, but this would worsen it's phase difference to the primary collimator. *KX1* in the horizontal plane is in a good position with respect to the target but unfortunately *KX2* is far from optimal with a phase difference of 88° to the target. Therefore a collimator of type 140° is missing in the x-plane which means that particles that are scattered inwards, i.e. towards the beam centre, can not be shadowed effectively. Moreover it is not possible to install an additional collimator of that type because the cold arc begins immediately downstream of *KX3*. However, protons scattered by a large angle > 100 μrad can still be captured with *KX3* which might be enough for sufficiently good background conditions.

Concerning the use of these secondary collimators one should be aware that HERA-B plans to install targets at all sides of the beam, i.e. above, below, left and right side of the beam. Therefore one needs secondary collimators from all sides as well. In the new setup there will be 16 jaws available and 11 of them have to be adjusted at the beam in each run (6 in the old setup). The increased number of collimators at the beam will complicate the optimization procedure considerably.

As one can see from the above estimations the risk of particle losses depends strongly on the phase difference between target and aperture limit. One can therefore minimize the background at the detectors by adjusting the phase advances slightly while keeping the integral machine tune constant. The investigation of such a phase bump is presently under way [4].

5. Conclusions

Protons that receive a large scattering angle at the HERA-B target can get lost immediately at an aperture restriction if there are no collimators which are optimized with respect to the target. For a typical situation in the 1994 experimental setup one would expect that 6 protons per 100 inelastic events in the HERA-B target hit the beampipe in the QR magnet upstream of ZEUS. As the desired (and achieved) interaction rate is of the order of 10 MHz or more this could easily explain the observed increased loss rates at ZEUS.

In the future setup the situation will be somewhat relaxed due to a smaller β function at the target position. Certain collimators in the section WL can be used as secondary collimators for the target. However, the setup of secondary collimators with respect to the target is not optimal. The adjustment of nearly the double number of jaws at the beam will take a much longer time. This is especially regrettable at the beginning of a run because then the machine delivers usually the peak luminosity which cannot be used during movements of collimator jaws.

A different possibility to minimize background is to pass a very large part of the scattered protons through critical aperture restrictions at the detectors. This may be achieved by adjusting the individual phase differences with a special quadrupole bump for ZEUS and H1. Again the usage of that possibility will complicate the machine operation.

In general it will be important to gain more experience on the influence of the target on the background situation during the experimental tests in 1995. Especially the interaction of targets and collimation system should be investigated as a function of the collimator setup.

6. References

[1] P.V. Murthy et al., Nucl. Phys. B 92 (1975) 269
[2] T.J. Roberts et al., Nucl. Phys. B 159 (1979) 56
[3] G. Belletini et al. Nucl. Phys. 79 (1966) 609
[4] B. Holzer, private communication
[5] B. Parker, internal note, to be published
[6] M. Seidel, DESY 94-103 (1994)